Monotropic Liquid Crystal Behavior in Two Poly(ester imides) with Even and Odd Flexible Spacers

Ricardo Pardey, Anqiu Zhang, Patricia A. Gabori, Frank W. Harris, and Stephen Z. D. Cheng*

Institute and Department of Polymer Science, College of Polymer Science and Polymer Engineering, The University of Akron, Akron, Ohio 44325-3909

Jerry Adduci and John V. Facinelli

Department of Chemistry, Rochester Institute of Technology, Rochester, New York 14623-0887

Robert W. Lenz

Department of Polymer Science and Engineering, University of Massachusetts, Amherst, Massachusetts 01003

Received March 18, 1992; Revised Manuscript Received June 1, 1992

ABSTRACT: Mesophase behavior of two poly(ester imides) synthesized from *N*-[4-(chloroformyl)phenyl]-4-(chloroformyl)phthalimide and 1,4-butanediol or 1,9-nonanediol has been extensively studied. One of the polymers has four methylene units (even) and the other nine methylene units (odd) in its respective flexible spacers. Both polymers show monotropic liquid crystal behavior which has been identified by differential scanning calorimetry (DSC), wide-angle X-ray diffraction (WAXD), and polarized light microscopy (PLM) experiments. The liquid crystal phase seems to be more ordered than the nematic phase. Further crystallization from this liquid crystal phase can be achieved during cooling and/or isothermal experiments below the isotropic melt to liquid crystal transition temperature. This indicates that the molecules in the liquid crystal phase possess high mobility. Isothermal experiments on these polymers at temperatures above the monotropic liquid crystal transition lead to direct crystallization from the isotropic melt with large axilitic or spherulitic texture.

Introduction

Liquid crystal polymers have become an increasingly active field of academic and industrial research. Academically, they offer various phase transitions for study. Industrially, fibers, films, coatings, and molding materials with remarkable mechanical and optical properties are made from the oriented anisotropic phase of these polymers.

The key to liquid crystal formation is geometric anisotropy. Molecules must be either "rodlike" or "disklike" in order to preferentially orient themselves in the liquid crystal phase. One major class of liquid crystal polymers is the thermotropic, main-chain mesogen–nonmesogen type,[1-29] in which the rigid mesogens are separated by flexible spacers. For the rigid mesogens, a traditional question is always how rigid and how big a mesogenic group must be in order to stabilize orientational order. This is associated with size, polarity, rigidity, and anisotropic geometry of the mesogen. On the other hand, it has also been recognized that some type of flexible spacers, such as methylene spacers, play an active role in the orientational order of the liquid crystal phase,[6,7,30-33] and others such as ethylene oxide spacers only act as diluents in the system.[23] For the methylene spacers, a parity (odd–even) effect also significantly affects the orientational order.[30-33]

The liquid crystal phase can also be either enantiotropic or monotropic. Enantiotropic phases are thermodynamically stable in a temperature region between the crystal melting temperature (T_d) and the isotropization temperature (T_i). Monotropic phases, however, are only stable at temperatures below the crystal melting. Experimentally, the monotropic phase can be observed on cooling provided that the crystallization process is bypassed due to supercooling. The recognition of monotropic phases can be traced as far back as 1877.[34] From a thermodynamic point of view, as discussed in ref 35, one can readily understand the monotropic phase through a diagram of Gibbs free energy of the different phases versus temperature. If kinetics causes a crystallization process to be bypassed during cooling, a liquid crystalline phase appears at a temperature of T_d, which is below T_m, and further crystallization may occur below this temperature.

Monotropic liquid crystal phases have been widely reported in small molecule liquid crystals as early as 1923.[36] Recently, it has also been found that monotropic phases exist in polymer liquid crystals, such as a family of polyethers and copolyethers synthesized by Percec's research group.[37-43] In the polyethers synthesized from 1-(4-hydroxyphenyl)-2-(2-methyl-4-hydroxyphenyl)ethane and α,ω-dibromoalkanes (MBPE), it has been observed that the monotropic phase only exists for the polyethers containing odd numbers of methylene spacers. Furthermore, this phase transition from the isotropic melt is mainly attributed to the ordering process of the methylene spacers rather than the semiflexible mesogen.[42,43] On the other hand, for the MBPE copolyethers, due to the irregularity of chemical structure, the crystallization process is hampered and the monotropic liquid crystal phase can thus be further stabilized over a wide range of temperatures.[37-40]

In this paper, we report phase behavior of two polymers of a series of poly(ester imides) in which the number of methylene spacers varies from 4 to 10 and 12. These poly(ester imides) were synthesized from *N*-[4-(chloroformyl)phenyl]-4-(chloroformyl)phthalimide and the respective diols by solution polymerization in refluxing 1,2,4-trichlorobenzene (TCB). The chemical structures of the repeat units are

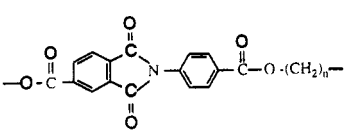

* To whom correspondence should be addressed.

0024-9297/92/2225-5060$03.00/0 © 1992 American Chemical Society

The polymers are abbreviated as PEIM(n), where n represents the number of methylene units in the structure. It should be noted that this family of PEIM(n) has the same chemical structure as one of those synthesized by Kricheldorf et al.[24-29] They found that PEIMs form a crystalline state with a layered supermolecular order, a so-called crystalline smectic state. In addition, PEIM(n=even)s can form a smectic glass. After crystal melting, all PEIMs exhibit the isotropic state. No monotropic liquid crystal behavior has been discussed.[26,28] The two polymers discussed in this paper are PEIM(n=4) with an even number and PEIM(n=9) with an odd number of methylene units in the spacers. It should be noted that in these polymers the mesogenic structure is asymmetric. Head-to-head and head-to-tail sequences are randomly distributed along the polymer chains. It is interesting to observe that both of these polymers show monotropic liquid crystal phases. Their phase structures, transitions, and morphologies are discussed. This discussion leads to a speculation of the origin of the orientation in the mesophase of these polymers.

Experimental Section

Materials and Samples. The synthesis of PEIM involved coupling of *N*-[4-(chloroformyl)phenyl]-4-(chloroformyl)phthalimide and the respective diols, with the number of methylene groups (n) varying from 4 to 10 and 12. The detailed synthetical procedure will be reported elsewhere.[44] In brief, in the monomer synthesis, 4-aminobenzoic acid (82.3 g, 0.600 mol) was dissolved in dimethylacetamide (DMAc) (336 mL) in a three-neck 100-mL round-bottom flask equipped with a condenser, magnetic stirrer, thermometer, and nitrogen inlet tube. The contents were cooled to 273 K while nitrogen was bubbled through. Trimellitic anhydride (TMA, 115.2 g, 0.600 mol) was added, and the solution was stirred overnight (18 h) at room temperature. Acetic anhydride (108 mL, 117 g, 1.14 mol) and pyridine (25 mL, 25 g, 0.31 mol) were added to the flask. The contents were heated at 427 K for 5 h. After cooling overnight, a fine white solid precipitated from the solution. The solid was collected by filtration, washed with cold acetone, and dried in vacuum at 363 K for 20 h to give 135.1 g with a yield of 72.3%. The product was recrystallized from dimethylformamide (DMF), filtered, and dried in vacuum at 353 K for 12 h with a melting point of 641–645 K.

Thionyl chloride (100 mL, 165 g, 1.39 mol) was placed in a round-bottom flask equipped with a nitrogen inlet and a reflux condenser with a drying tube. *N*-[4-(chloroformyl)phenyl]-4-(chloroformyl)phthalimide (33.0 g, 0.106 mol) and 10 drops of DMF were added, and the heterogeneous mixture was heated to reflux for 8 h. After cooling, the product precipitated and was collected by filtration, washed with *n*-hexane, and dried in vacuum at 353 K for 8 h. The product was purified by precipitation from benzene into *n*-hexane, filtered, and dried in vacuum again at 353 K for 10 h. A second purification gave 19.8 g with a yield of 54% and a melting point of 448–450 K. The products used in this study were analyzed by elemental analyses and NMR and infrared spectroscopies to identify the chemical structures.

The polymers were prepared by solution polymerization. Equimolar amounts of bis(acid chloride), a dialcohol and 1,2,4-trichlorobenzene were placed in a 200-mL one-neck round flask with a heating mantle. The flask contents were heated at reflux with stirring until hydrogen chloride gas evolution ceased. This was noted by testing the gas outlet with universal pH paper. Upon cooling, the poly(ester imides) precipitated were filtered, washed with *n*-hexane or diethyl ether, and dried in vacuum at 353 K for 30 h.

Intrinsic viscosity measurements in *m*-cresol at 303 K indicate that for PEIM(n=4) and -(n=9) their intrinsic viscosities are 0.4 and 0.6 dL/g, and the molecular weights of their repeat units are 365 and 435 g/mol, respectively. For differential scanning calorimetry (DSC) measurements, typical sample weights were between 5 and 10 mg. For fast heating and cooling rates the sample weight was correspondingly decreased in order to avoid thermal lag. For example, at a rate of 40 K/min, the sample weight was only about 0.2 mg. Both powder and fiber patterns were obtained using wide-angle X-ray diffraction (WAXD) experiments. The PEIM fibers were melt spun and quenched to below their glass transition temperatures to suppress crystal formation. Solution cast films were used for polarized light microscopy (PLM) observations. The solvent was evaporated in a vacuum oven at 520 K for 5 h. Solid films with a thickness of about 10 μm were obtained.

Differential Scanning Calorimetry (DSC). Thermal measurements were carried out on a Perkin-Elmer DSC-2 and a Seiko DSC 210. The DSCs were calibrated with an indium standard at all heating and cooling rates used (0.5–40 K/min). All samples were run under a dry nitrogen atmosphere. They were heated to about 20 K above the melting temperature and held there for 2 min before each experiment. Nonisothermal experiments entailed quenching the sample from 20 K above its melting temperature to liquid nitrogen prior to heating at different rates. Isothermal experiments were conducted by quenching the molten sample to a preset temperature in the DSCs and recording the heat flow on a time basis. These samples were immediately heated at 10 K/min to above the melting temperature.

Sequential cooling and heating experiments were also performed. The samples were cooled at 10 K/min to a temperature slightly below the first exothermic transition peak and held there isothermally for a preset time. The samples were then reheated at 20 K/min.

Polarized Light Microscopy (PLM). An Olympus BH-2 PLM coupled to a Mettler FP82HT hot stage was used for morphological observations. Samples were heated to 20 K above the melting temperature and held there for 2 min, the same as in the DSC experiments. Nonisothermal experiments entailed cooling at 10 K/min to 325 K. Isothermal experiments consisted of quickly transferring the molten sample to a hot stage preset at the desired temperature and holding it there for various periods of time for morphological observations.

Wide-Angle X-ray Diffraction (WAXD). A Rigaku X-ray generator with a 12-kW rotating anode was used, and the point-focused beam was monochromatized to Cu Kα with a graphite crystal. X-ray powder diffraction data were recorded on a diffractometer. A temperature controller was attached to the WAXD apparatus. The precision of the controller was ±1 K in the temperature range studied. Nonisothermal experiments were carried out at a cooling rate of 5 K/min. Isothermal experiments were conducted by quickly transferring the molten sample to a preset temperature on the sample holder in the controller. The total time necessary to transfer the sample and collect the first X-ray scan was about 1 min. In both cases, thermal X-ray experiments were carried out parallel to the DSC experiments. The fiber patterns were obtained with a flat plate vacuum camera using a Rigaku tube X-ray generator. The d spacing was calibrated by silicon powder which shows a diffraction angle of 2θ = 28.46°.

Results

Phase Transitions Observed in DSC Experiments. Figure 1 shows two DSC heating traces. For liquid nitrogen quenched PEIM(n=4) samples, one can find the glass transition at T_g of 380 K. An exothermic peak at 440 K follows the glass transition with a heat of transition of 2.5 kJ/mol. After this transition, two major endothermic processes are observed. One occurs at 492 K and the other at 504 K, with heats of transitions of 3.5 and 5.0 kJ/mol, respectively. An exothermic transition between these two melting peaks seems to overlap with its neighboring processes, and it can be observed clearly at lower heating rates. For quenched PEIM(n=9) samples, the glass transition temperature is observed at 323 K. An exothermic peak overlaps and closely follows at around 335 K with a heat of transition of 7.9 kJ/mol. Immediately after, an endothermic transition at 384 K occurs with the same heat of transition. The difference between these two polymers seems to be in overall transition kinetics

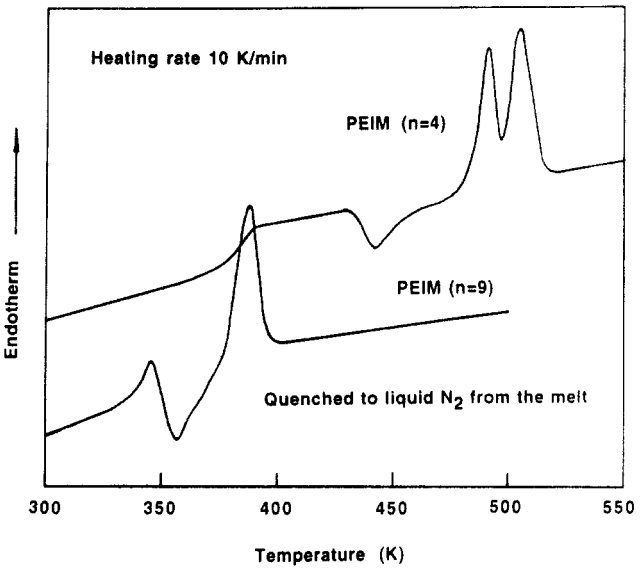

Figure 1. Set of DSC heating traces for quenched PEIM(n=4) and PEIM(n=9) at 10 K/min.

and temperatures. PEIM(n=9) transfers to an ordered phase much slower than PEIM(n=4) at lower transition temperatures.

When the samples are cooled from the melt to below their glass transition temperatures at different cooling rates, two exothermic peaks are usually observed for PEIM(n=4) (Figure 2a), and only one peak appears in PEIM(n=9) (Figure 2b). For PEIM(n=4), the second low-temperature exothermic peak shifts toward the high-temperature side with decreasing cooling rates. In contrast, the high-temperature peak remains almost invariable at a temperature of 500 K in this cooling rate range. When the cooling rate is slow enough, such as 2.5 K/min in Figure 2a, the two exothermic peaks become unresolvable. The heat of transition in this case represents the summation of both contributions of the low- and high-temperature exothermic peaks. Furthermore, the heat of transition contributed by the high exothermic peak is constant (3.1 kJ/mol), while that of the low-temperature exothermic peak decreases with increasing cooling rate. Table I gives the transition parameters for PEIM(n=4) at different cooling rates. For PEIM(n=9) (see Figure 2b and Table II), the cooling rate independent transition occurs at around 370 K with a heat of transition of 4.3 kJ/mol. In contrast to PEIM(n=4), a lower temperature exothermic peak is not observed.

Sequential cooling and heating experiments were carried out on both PEIM(n=4) and PEIM(n=9). Figure 3 shows the DSC traces for PEIM(n=4), as an example. After the samples are cooled to 490 K at 10 K/min, an immediate successive heating (0 min) leads to only one endothermic transition peak with the same onset transition temperature and the same heat of transition as those of the exothermic transition peak observed during cooling. As time increases, the heat of transition of the lower endothermic peak decreases while the peaks at higher temperatures gradually develop. After a certain time [6 min for PEIM(n=4) and 80 min for PEIM(n=9)], the first peak completely disappears and only the higher temperature peaks remain. Some crystal melting and recrystallization processes at higher temperatures for PEIM(n=4) can also be seen during heating, but they are not further discussed in this paper.

Isothermal Transition Kinetics Measured from DSC Experiments. The Avrami equation[45] is used to discuss the overall transition kinetics of these two samples. Figure 4 shows the DSC exothermic transitions when the samples of PEIM(n=4) and PEIM(n=9) are isothermally held at temperatures below and above the temperature where the first, exothermic transition during DSC cooling experiments appears. At lower isothermal temperatures the DSC traces show two different exothermic processes. For PEIM(n=4) the first transition appears at very short time scales (peak maximum is at 0.5 min), when compared to PEIM(n=9) (peak maximum is at 2 min). At higher isothermal temperatures, only one exothermic crystallization peak is observed for both polymers.

Figure 5 shows the relationship between log [-ln (1 - W_c)] versus log t_c at the corresponding isothermal temperatures for PEIM(n=9). When the sample is isothermally held at 373 K, the transition processes occur in two stages: the first short-time and the second long-time transition processes. Both processes are characterized by an Avrami dimensionality parameter of $n = 2$. At a higher isothermal temperature of 383 K a single process can be found with an Avrami dimensionality parameter of n = 3. On the other hand, the transition kinetics of PEIM(n=4) is also represented by a two-stage transition process at lower isothermal temperatures. However, the first transition stage is too fast to make a quantitative analysis due to the fact that the DSC has not reached its isothermal condition before the transition starts. The second transition stage possesses an Avrami dimensionality parameter of $n = 2.3$ at 453 K. When the sample is held isothermally at higher temperatures, a single process is observed with an Avrami dimensionality parameter of $n = 2.1$ at 513 K.

Structure Formations Observed through WAXD Experiments. Figure 6 shows nonisothermal WAXD results during cooling at 5 K/min. PEIM(n=4) exhibits an amorphous halo above its highest endothermic transition temperature (510 K). During cooling from 523 K to the first exothermic transition, the center position of the amorphous halo shifts to higher 2θ angles (lower d spacings). At the temperature which leads to the exothermic transition observed by DSC, only one weak diffraction peak is observed in a 2θ region below 10°. Another very weak peak between 10° and 20° may also be seen. These peaks correspond to the meridian diffraction spots in the fiber pattern (see below). During further cooling, where the second lower exothermic transition in DSC is observed, the diffraction peaks start developing. For PEIM(n=9), a similar situation can be observed during cooling to the first exothermic transition. However, upon further cooling no diffraction peaks are observed. A long annealing time is necessary for the development of an ordered structure. If one plots the change in d spacing with respect to temperature during cooling for these two polymers, as shown in Figure 7, the drops in d spacings evidently correspond to the temperatures where the first, higher exothermic transitions are detected in the DSC cooling experiments.

The isothermal temperatures are chosen to be slightly below the temperatures at which the first, higher exothermic transition is observed in DSC cooling experiments. Figure 8 shows the WAXD data for PEIM(n=9). The diffraction pattern initially shows two weak diffraction peaks, and the average intermolecular spacing is close to those of the amorphous samples. Crystal diffraction peaks for PEIM(n=9) develop in approximately 80 min, while those of PEIM(n=4) develop within 6 min.

Figure 9 shows the WAXD fiber patterns. Both parts of Figure 9 exhibit a relatively diffuse spot along the equatorial and two sharp spots along the meridian direction. These meridian diffractions correspond to d

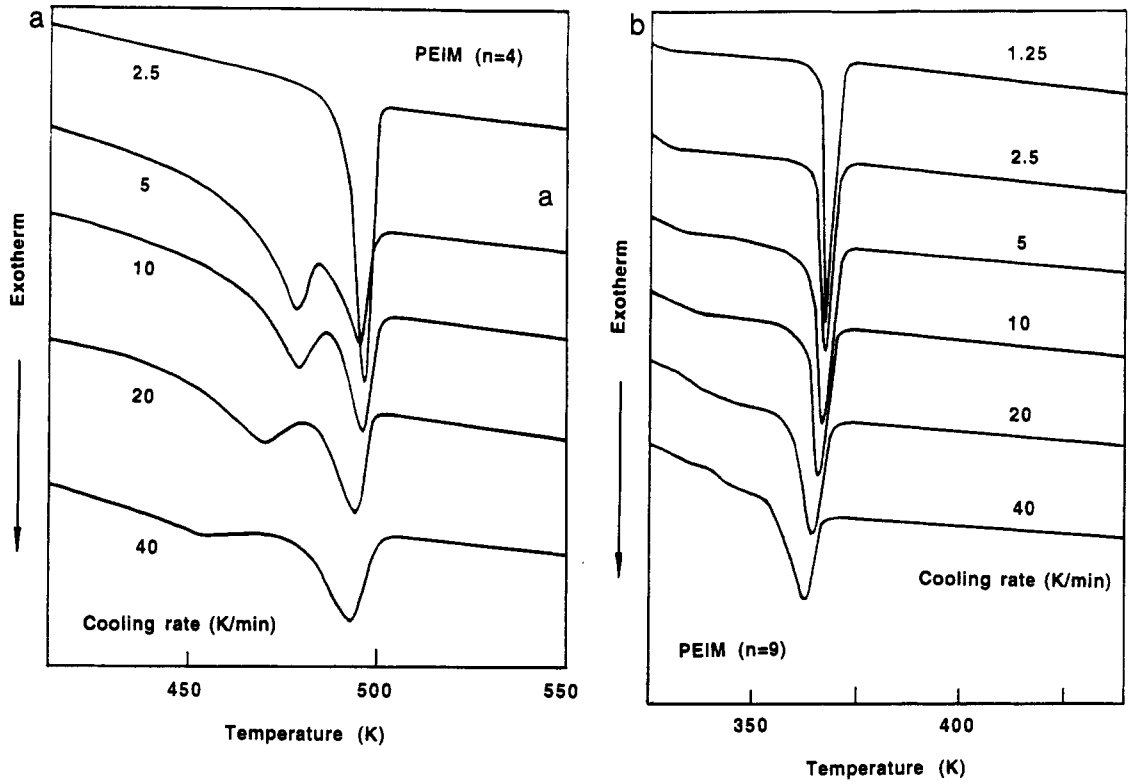

Figure 2. Sets of DSC cooling traces for PEIM(n=4) (a) and PEIM(n=9) (b) from the isotropic melt at different cooling rates.

Table I
Heats and Temperatures of Transitions of PEIM(n=4) at Different Cooling Rates

cooling rate (K/min)	T_1 (K)	ΔH_1 (kJ/mol)	T_2 (K)	ΔH_2 (kJ/mol)	ΔH_{tot} (kJ/mol)
5	501.4	-3.1	479.4	-4.4	-7.5
10	500.1	-3.1	479.8	-3.5	-6.6
20	500.0	-3.1	472.3	-3.4	-6.5
40	498.3	-3.0	broad	-2.1	-5.1

Table II
Heats and Temperatures of Transitions of PEIM(n=9) at Different Cooling Rates

cooling rate (K/min)	T_1 (K)	ΔH_1 (kJ/mol)	cooling rate (K/min)	T_1 (K)	ΔH_1 (kJ/mol)
1.25	369.2	-4.3	10	367.0	-4.3
2.5	369.2	-4.4	20	365.1	-4.3
5.0	368.1	-4.4	40	363.0	-4.3

spacings of 0.6 and 1.6 nm for PEIM(n=4) and 0.6 and 2.2 nm for PEIM(n=9). The diffraction spots along the meridian direction are also observed in the WAXD powder diffraction patterns (Figures 6 and 8).

Morphological Observation from PLM. During cooling the samples of PEIM(n=4) and PEIM(n=9) from the melt in the hot stage at 10 K/min, birefringent patterns develop within seconds at 500 and 370 K, respectively. The morphological textures are shown in Figure 10. Clear disclination points or "threadlike" textures can be observed. Immediate reheating leads to a disappearance of the texture only a few kelvin higher than 500 and 370 K for these two polymers. Further cooling leads to a slight change of the texture toward tiny and grainy patterns. On the other hand, in isothermal experiments at temperatures of 518 K for PEIM(n=4) and 403 K for PEIM(n=9), which are above their first, exothermic transition temperatures observed in DSC during cooling mature axialites and spherulites are clearly developed. Note that the axialitic growth is two-dimensional. In addition, PEIM(n=9) shows two different types of spherulites. The one with low birefringence melts at 423 K, and the other, with

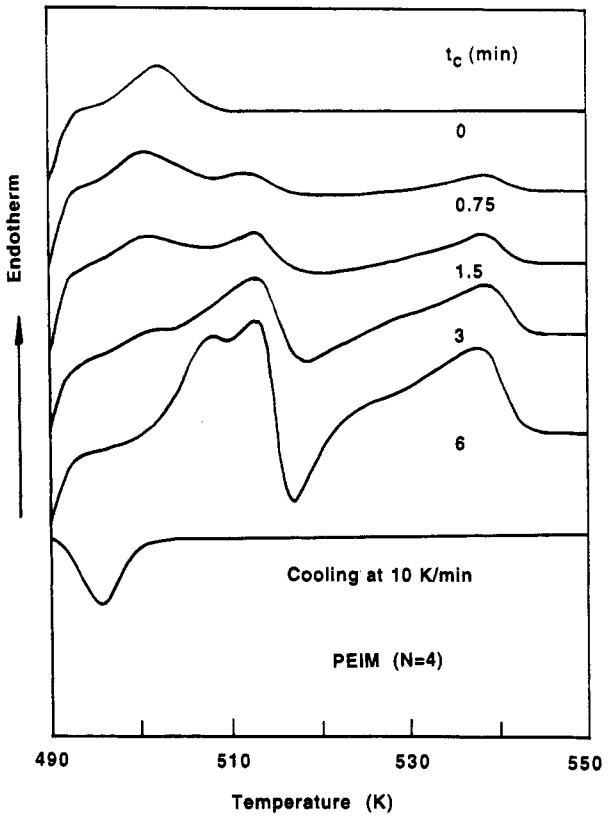

Figure 3. Set of melting traces of PEIM(n=4) isothermally held at 490 K for different times after cooling at 10 K/min from isotropic melt.

a characteristic ring pattern and high birefringence, melts at 463 K. When the isothermal temperatures are below those of the first exothermic transition temperatures during cooling, both polymers exhibit morphological textures similar to those shown in Figure 10. If one quenches a sample of PEIM(n=4) which has previously been isothermally held at 518 K to below 500 K, two different morphologies now coexist. These are spheru-

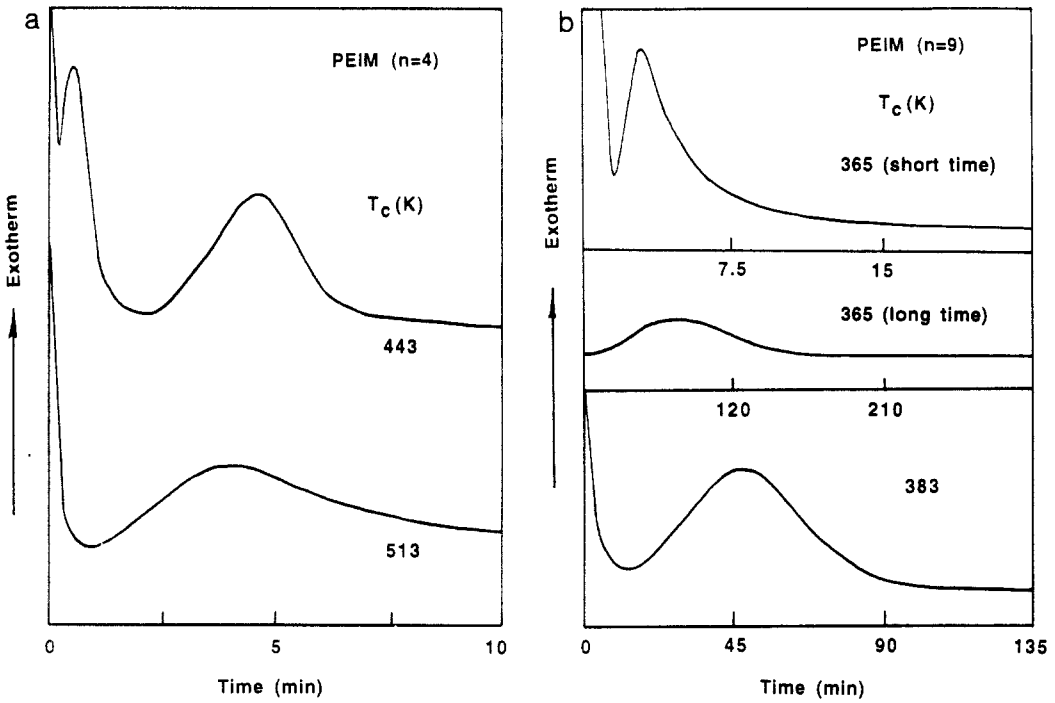

Figure 4. (a) Set of DSC exothermic traces of PEIM(n=4) isothermally kept at 453 and 513 K. (b) Set of DSC exothermic traces of PEIM(n=9) isothermally kept at 365 and 383 K.

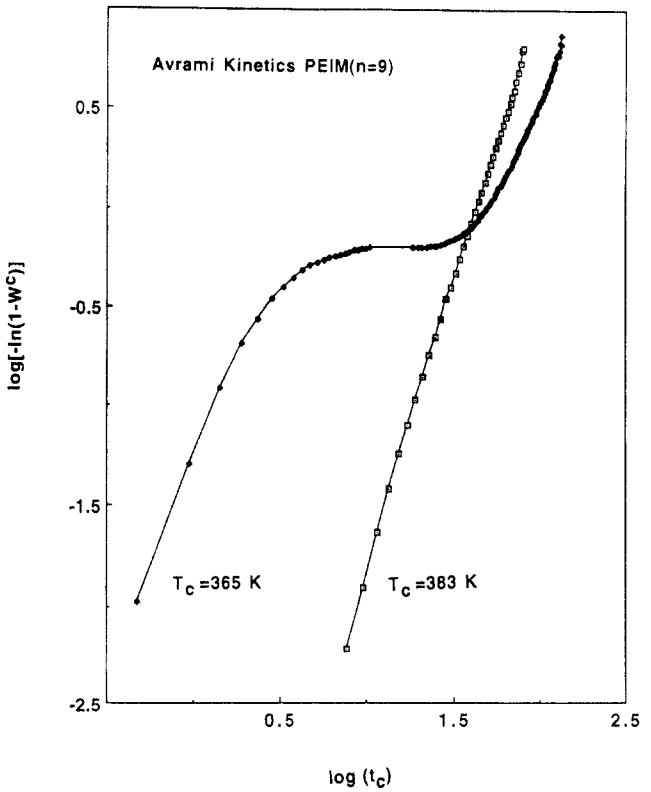

Figure 5. Avrami relationship between log [−ln (1 − W_c)] and log t_c for PEIM(n=9) isothermally kept at 365 and 383 K.

lites crystallized at 518 K, and threadlike textures formed during the quenching. Successive heating, again, leads to a melting of the threadlike texture at 500 K.

Discussion

We have reported a number of experimental observations obtained through DSC, WAXD, and PLM methods for the phase behavior of two poly(ester imides): PEIM(n=4) and PEIM(n=9). If we concentrate our attention on their monotropic mesophase transition behavior, the experimental observations can be summarized as follows: (1) During cooling, the first, higher temperature exothermic transitions observed through DSC experiments are independent of the cooling rate (0.5–40 K/min), with the heats of transitions of 3.1 kJ/mol for PEIM(n=4) and 4.3 kJ/mol for PEIM(n=9). (2) Sequential cooling and heating experiments indicate that these first, higher temperature transitions do not exhibit supercooling, revealing that the transitions are close to equilibrium. (3) Isothermal kinetics studies show that when the polymers are held at temperatures below the first transition during cooling, two different stages of the exothermic processes are observed. However, if the samples are kept at higher temperatures, only a single, exothermic process occurs. The Avrami dimensionality parameters for the two-stage processes are around 2, and that for a single process is dependent upon the growth dimensionality (2 for axialites and 3 for spherulites). (4) WAXD experiments only show weak diffraction peaks in quenched samples. They correspond to the diffraction spots along the meridian direction in the fiber pattern. A drop in the d spacing for each polymer is evident at the first exothermic transition temperature. Only further cooling to lower temperatures allows the crystals to develop. (5) PLM observations reveal threadlike textures or disclination points for both polymers. These reveal that at least some degree of order has been introduced during the first exothermic transitions.

A detailed discussion may start with the type of order involved in the first exothermic transition. DSC cooling results indicate that the transition possesses a cooling rate independence (Figure 2). From the WAXD powder pattern, only weak diffraction peaks are generated through the transition during cooling (Figures 6) or in the initial stage of isothermal WAXD experiments (Figure 8). The drop observed in the d spacing which represents the average lateral distance between chain molecules is evident (Figure 7). Finally, the threadlike texture is observed through PLM (Figure 10). These experimental observations lead to the identification of a liquid crystal phase.[46,47] This is further confirmed by the WAXD fiber pattern (Figure 9), which clearly indicates that only orientational order exists with some layer structures. The sharp

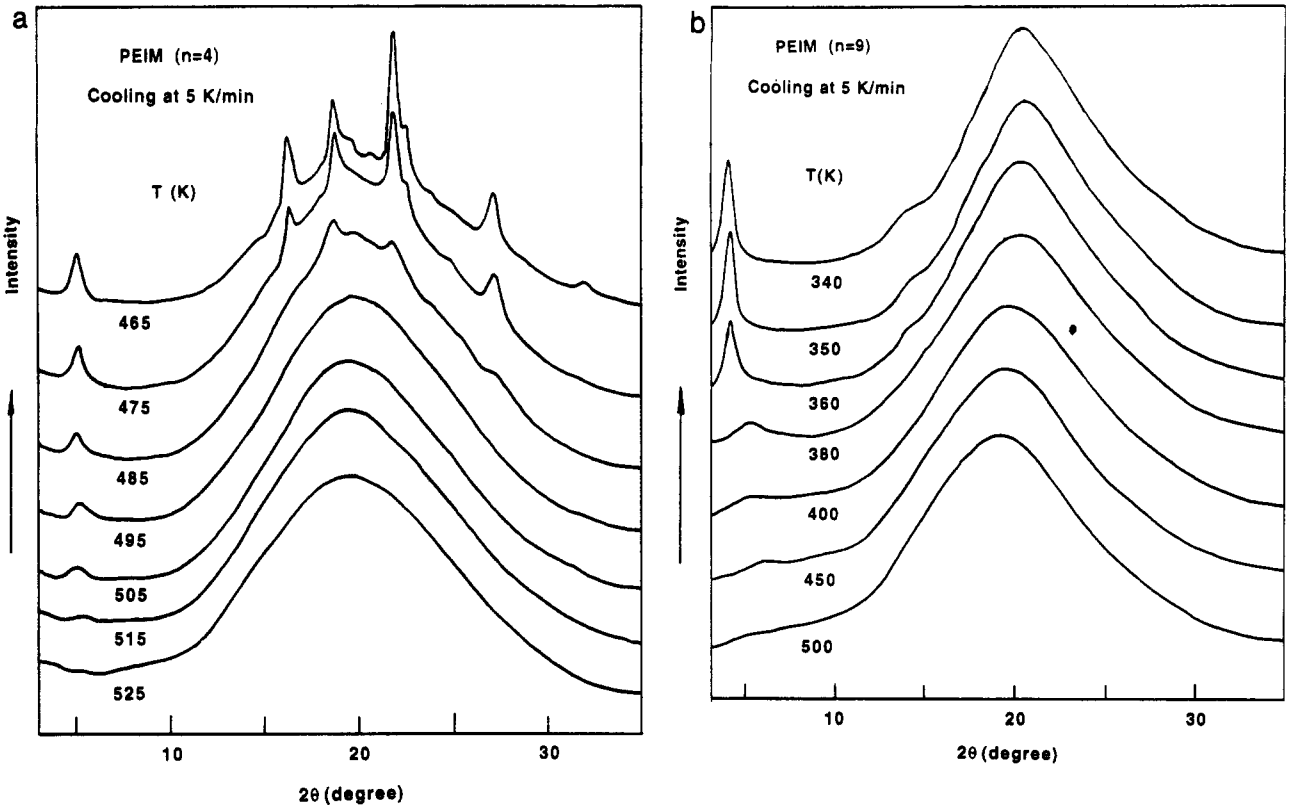

Figure 6. (a) WAXD powder pattern of PEIM(n=4) samples cooled at 5 K/min from the isotropic melt. (b) WAXD powder pattern of PEIM(n=9) samples cooled at 5 K/min from the isotropic melt.

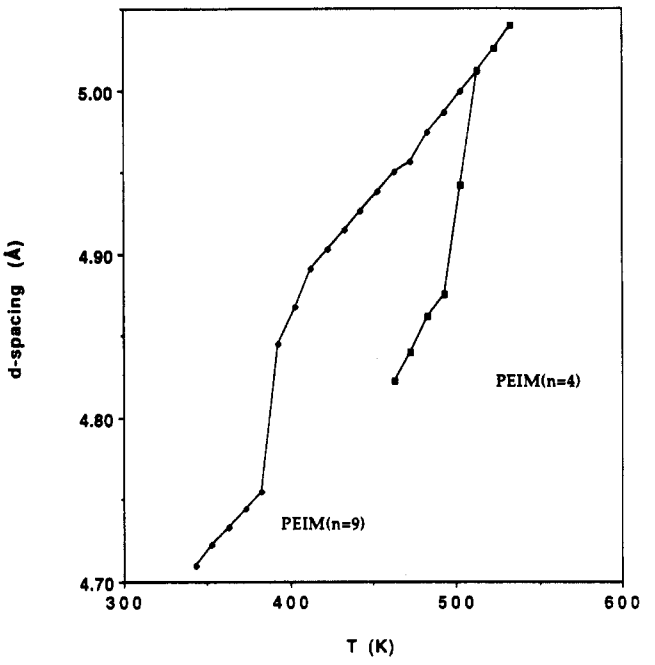

Figure 7. WAXD d spacings for both polymers as a function of temperature.

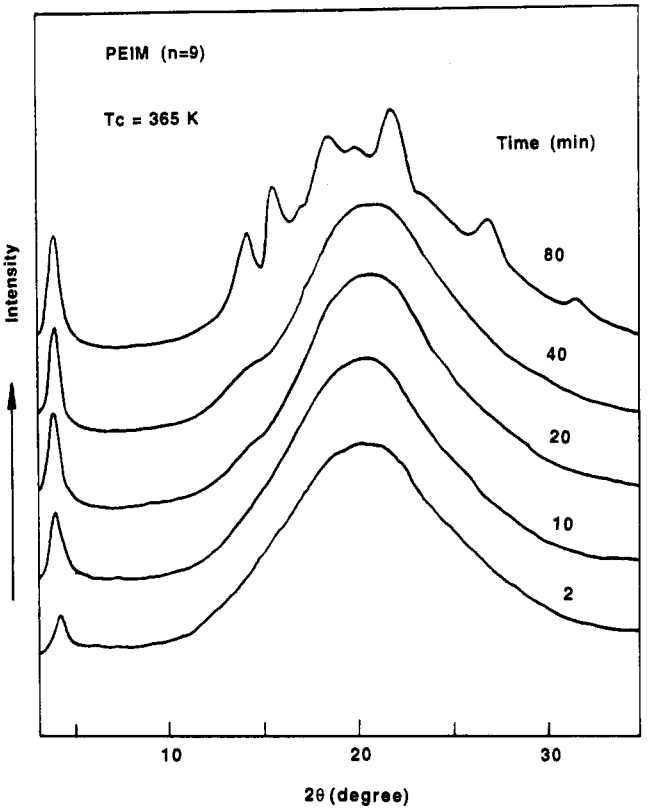

Figure 8. WAXD powder pattern of PEIM(n=9) isothermally kept at 365 K for different times.

diffraction spots along the meridian with d spacings of about 0.6 nm for both PEIM(n=4) and PEIM(n=9) are interesting since this d spacing represents the length of a trans conformation of the methylene units in PEIM(n=4), but it does not correspond to that in PEIM(n=9). This might possibly be an indication that in the flexible spacer with an odd number of methylene units some gauche conformations could exist and/or the units could be tilted. Another possibility could be that this 0.6-nm d spacing might be attributed to the common mesogen in the polymers. However, a definitive conclusion cannot be reached until detailed ^{13}C solid-state nuclear magnetic resonance experiments are conducted. The second spot on the meridian with a d spacing of 2.2 nm for PEIM(n=9) and 1.7 nm for PEIM(n=4) is roughly the repeat unit lengths of both polymers. They are corroborated by computer modeling, adopting the minimum rotational potential conformations.[48] Since the meridian diffraction spots give information about the one-dimensional liquid

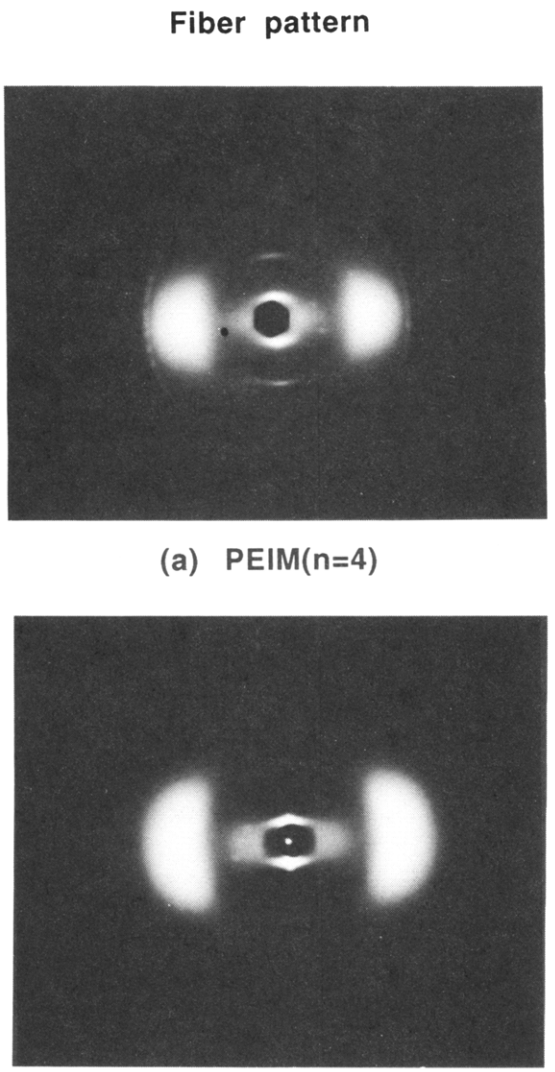

Figure 9. (a) WAXD fiber pattern of PEIM(n=4) quenched from the isotropic melt. (b) WAXD fiber pattern of PEIM(n=9) quenched from the isotropic melt.

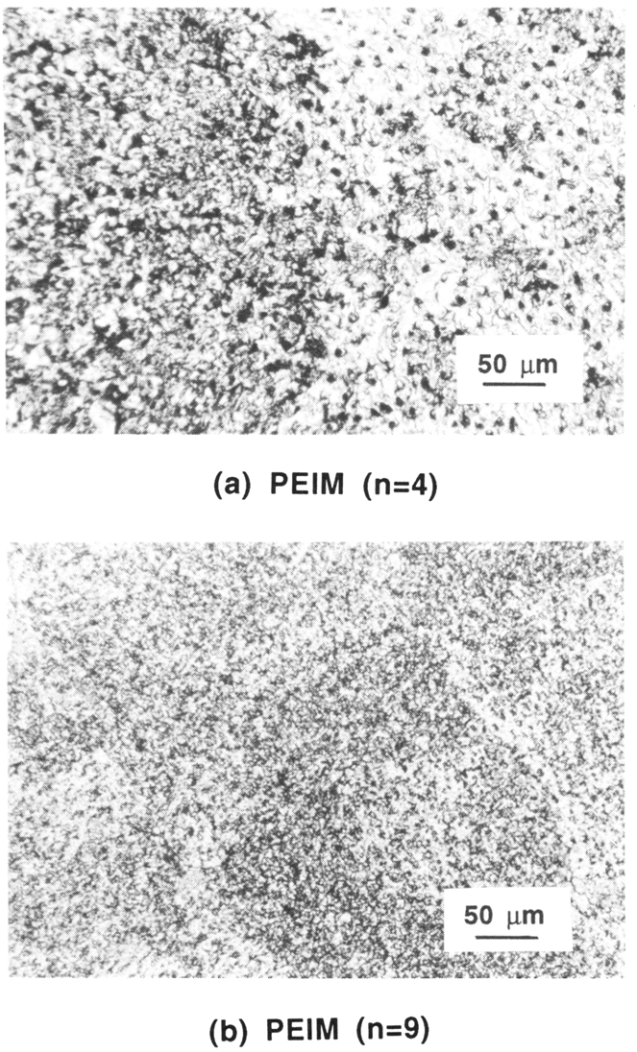

Figure 10. Threadlike texture of PEIM(n=4) (a) and PEIM-(n=9) (b) cooled at 10 K/min to below their first exothermic transition peaks shown in DSC.

crystal periodicity of the oriented fibers, two possibilities may exist. Namely, these two diffraction spots in each polymer represent a single one-dimensional lattice or two different lattices. In the former case the samples are homogeneous, and in the latter case, spacers and mesogens are in different mesophase systems. Overall, the order in the liquid crystal phase in these two polymers seems to be more ordered than the nematic state. For the same set of polymers, Kricheldorf et al. reported that PEIM-(n=even)s can form smectic glass and a crystalline smectic phase.[26,28]

These liquid crystal phases can undergo further crystallization during cooling or isothermal experiments. At isothermal temperatures below the formation of the liquid crystal phase, two different transitions are observed: first, the monotropic liquid crystal transition and, second, crystallization from the liquid crystal phase. It is interesting to observe that the Avrami dimensionality parameters are around 2. Note that for oriented rigid polymers growing longitudinally, the Avrami treatment can be satisfied as a two-dimensional growth if molecules are all parallel. The parameter n must be 2 in the case of predetermined nuclei.[49] At isothermal temperatures above this liquid crystal transition, crystallization occurs directly from the isotropic melt. This gives the axilitic or spherulitic texture, with an Avrami dimensionality parameter of either 2 or 3 under an athermal nucleation condition. In this case the supercooling in not sufficient to allow the material to reach the liquid crystal phase. The application of the Avrami equation, however, assumes that the growing centers should not interact strongly with one another and should in addition have been initiated at the same instant (in an athermal case).

It is also interesting that both polymers containing an even and an odd number of methylene units in their flexible spaces show the monotropic liquid crystal behavior. In our previous publications for the study of a family of MBPE polyethers, only those which have an odd number of methylene units exhibit this behavior.[41,42] On the other hand, a series of MBPE copolyethers has been reported to display monotropic liquid crystal behavior.[39,40] It has been known that the stabilization of a liquid crystal phase is critically associated with rigidity, size, and structural symmetry of mesogenic groups in polymers. In the present case, the mesogenic group is rigid, but its chemical structure is asymmetric (head-to-head and/or heat-to-tail random configurations). A noncoplanar conformation between the phenylene ring and imide group in the mesogen is also found through computer modeling (45° rotational angle gives the minimum potential energy level).[48] These factors may affect the molecular packing and orientational order in the liquid crystal phase, and lead to an increase in the Gibbs free energy of this state (less stable). This pushes

the transition temperature between the liquid crystal phase and isotropic melt toward a lower temperature which is even below the crystal melting temperature. As a result, a monotropic liquid crystal is formed.

Observation of this monotropic phase is, however, largely dependent upon the capability of crystallization in these systems. In this case, the asymmetric chemical structure in the mestogenic group also plays an important role since a deep suppression of crystallization allows formation of this monotropic liquid crystal phase (staying in the liquid crystal phase longer) during cooling.[35] Copolymers may also hamper the crystallization as in some of the MBPE copolyethers, and therefore, the liquid crystal phase may be stabilized in the entire temperature region between glass transition and isotropization temperatures.[39,40] It has also been noticed that PEIM(n=9) crystallizes much slower than PEIM(n=4) does (Figures 4 and 5). This cannot be explained by the change of rigidity in the polymers, but rather by the parity effect on different degrees of orientational order and chain packing in the liquid crystal phases, such as a possibility of gauche conformations involved in the methylene units.

When we further study the heats of transitions of the first, exothermic transitions for these two poly(ester imides), it is clear that increasing the number of methylene units from four to nine yields a heat of transition change from 3.1 to 4.3 kJ/mol (Tables I and II). This indicates that the methylene units at least partially contribute to the heats of transitions. If only the mesogen was attributed to the heat of transition and the methylene units acted only as diluent, the heats of transition of these two polymers would be close to each other, as in the case of poly(azomethine ethers) in which ethylene oxides are used as flexible spacers.[23] This experimental result thus provides an additional confirmation of the effect of methylene units on orientational order in the liquid crystal phase.[6,7,30-33] An example was reported by Blumstein and Thomas[6] and Blumstein and Blumstein[7,33] on a series of 4-4′-dihydroxy-2,2′-dimethyl-1,1′-azoxydibenzene–alkanedioic acid (ME9-S(n)) polymers. The contributions to the heat of transition of the mesogenic group with even and odd methylene units are 4.7 and 0.94 kJ/mol, respectively. They are very much parity dependent primarily due to the difference in their orientation caused by conformations of methylene units in the flexible spacers. Their corresponding entropy changes for ME9-S(n=even) are 7.55 J/(K/mol of mesogenic groups), and those of ME9-S(n=odd) are 1.41 J/(K/mol of mesogenic groups). However, the contributions to the heat of transition from methylene units are essentially closed: 0.16 versus 0.19 kJ/mol, and their entropy changes are 0.87 and 0.57 J/(K/mol of methylene units), respectively. On the other hand, in a series of MBPE with an odd number of methylene units in the spacers the enthalpy contribution to the orientational order per mole of mesogenic groups during the transition is only about 0.11 kJ/mol, while the entropy contribution is 1.3 J/(K/mol of mesogenic groups), which is similar to that in ME9-S(n=odd) polymers. Note that they are similar to the entropy change values in small molecule liquid crystal transitions at T_i.[50] For methylene spacers, the heat of transition per mole of methylene units is about 0.64 kJ/mol and its entropy of transition is 1.7 J/(K/mol of methylene units) which are substantially higher than those in the case of ME9-S(n). These observations indicate that the order in methylene units varies over a wide range for liquid crystal phases.

Turning back to the PEIM polymers, if assuming that the entropy contribution of the mesogenic groups at the transition is around 1 J/(K mol) for PEIM(n=9), which is slightly lower than those of the cases of MBPE(n=odd) and ME9-S(n=odd) polymers, the enthalpy contribution of the mesogenic groups at the transition is thus around 0.37 kJ/mol. This leads to an enthalpy change of 0.33 kJ/mol of methylene units. As a result, this enthalpy change contributed through methylene units during the transition is between those of the cases of ME9-S(n=odd) and MBPE(n=odd). We expect that the orientational order contributed by the mesogenic groups with both odd and even numbers of methylene units may not be as much different as in ME9-S(n) polymers due to the irregularity of the mesogenic structure and the noncoplanar conformation between the phenylene ring and the imide group.[43] If these speculations are held, one may consider that the parity dependence of the transition behavior in PEIM polymers could be mainly attributed to the methylene units. Nevertheless, the study of the whole family of poly(ester imides) is necessary to understand the contributions of the mesogenic group and the methylene units to the liquid crystal transition behavior.

Conclusion

PEIM(n=4) and PEIM(n=9) have shown an accessible monotropic liquid crystal phase during cooling. This phase is identified through the ordered structure development, thermal transition behavior, and morphological studies, and it is more ordered than the nematic phase. Further crystallization can be carried out for both polymers by cooling or annealing below the temperatures at which transitions from their isotropic melts to the liquid crystal phases occur. Nevertheless, the transition kinetics differ by about 1 order of magnitude due to the odd–even effect in the methylene units. Only by keeping both polymers isothermally above these transition temperatures can the crystals grow directly from the melt. A discussion of the contributions of mesogenic groups and flexible spacers to the liquid crystal transitions is also offered.

Acknowledgment. This work was supported by SZDC's Presidential Young Investigator Award from the National Science Foundation (Grant DMR-9157738) and Exxon Education Foundation.

References and Notes

(1) Ruviello, A.; Sirigu, A. *J. Polym. Sci., Polym. Lett. Ed.* **1975**, *13*, 455; *Eur. Polym. J.* **1979**, *15*, 61; **1979**, *15*, 423; *Makromol. Chem.* **1982**, *183*, 895.
(2) Jackson, W. J., Jr.; Kuhfuss, H. J. *J. Polym. Sci., Polym. Chem. Ed.* **1976**, *14*, 2043.
(3) Menrisse, P.; Noel, C.; Monnerie, L.; Fayolle, B. *B. Polym. J.* **1981**, *13*, 55.
(4) Griffin, A. C.; Havens, S. J. *J. Polym. Sci., Polym. Phys. Ed.* **1981**, *19*, 951.
(5) Anton, S.; Lenz, R. W.; Jin, J. I. *J. Polym. Sci., Polym. Chem. Ed.* **1981**, *19*, 1901.
(6) Blumstein, A.; Thomas, O. *Macromolecules* **1982**, *15*, 1264.
(7) Blumstein, R. B.; Stickles, E. M.; Blumstein, A. *Mol. Cryst. Liq. Cryst.* **1982**, *82*, 205.
(8) Blumstein, A.; Vilasagar, S.; Ponrathnam, S.; Clough, S. B.; Maret, G. *J. Polym. Sci., Polym. Phys. Ed.* **1982**, *20*, 877.
(9) Krigbaum, W. R.; Astar, J.; Toriumi, H.; Ciferri, A.; Preston, J. *J. Polym. Sci. Polym. Lett. Ed.* **1982**, *20*, 109.
(10) Krigbaum, W. R.; Watanabe, J. *Polymer* **1983**, *24*, 1299.
(11) Lenz, R. W.; Jin, J. I. *Macromolecules* **1981**, *14*, 1405.
(12) Ober, C. K.; Jin, J. I.; Lenz, R. W. *Polym. J.* **1982**, *14*, 9.
(13) Lenz, R. W. *Faraday Discuss. Chem.* **1985**, *79*, 21.
(14) Sigaud, G.; Yoon, D. Y.; Griffin, A. C. *Macromolecules* **1983**, *16*, 875.
(15) Viney, C.; Yoon, D. Y.; Reck, B.; Ringsdorff, H. *Macromolecules* **1989**, *22*, 4088.
(16) Moore, J. S.; Stupp, S. I. *Macromolecules* **1987**, *20*, 273, 282; **1988**, *21*, 1222.

(17) Stupp, S. I.; Moore, J. S.; Martin, P. G. *Macromolecules* **1988**, *21*, 1228.
(18) Jonson, H.; Werner, P.-E.; Gedde, U. W.; Hult, A. *Macromolecules* **1989**, *22*, 1683.
(19) Smyth, G.; Vallés, E. M.; Pollack, S. K.; Grebowickz, J.; Stenhouse, P. J.; Hsu, S. L.; MAcknight, W. J. *Macromolecules* **1990**, *23*, 3389.
(20) Laus, M.; Caretti, D.; Angeloni, A. S.; Calli, G.; Chiellini, E. *Macromolecules* **1991**, *24*, 1459.
(21) Aharoni, S. M. *Macromolecules* **1988**, *21*, 1941; **1989**, *22*, 686; **1989**, *22*, 1125.
(22) Aharoni, S. M.; Correale, S. T.; Hammond, W. B.; Hatfield, G. R.; Murthy, N. S. *Macromolecules* **1989**, *22*, 1137.
(23) Cheng, S. Z. D.; Janimak, J. J.; Sridhar, K.; Harris, F. W. *Polymer* **1989**, *30*, 494; **1990**, *31*, 1122.
(24) de Abajo, J.; de la Campa, J.; Kricheldorf, H. R.; Schwarz, G. *Makromol. Chem.* **1990**, *191*, 537.
(25) Kricheldorf, H. R.; Huner, R. *Makromol. Chem., Rapid. Commun.* **1990**, *11*, 211.
(26) Kricheldorf, H. R.; Domschke, A.; Schwarz, G. *Macromolecules* **1991**, *24*, 1011.
(27) Kricheldorf, H. R.; Jahnke, P. *Eur. Polym. J.* **1990**, *9*, 1009.
(28) Kricheldorf, H. R.; Schwarz, G.; de Abajo, J.; de la Campa, J. G. *Polymer* **1991**, *32*, 942.
(29) Kricheldorf, H. R.; Huner, R. *J. Polym. Sci., Polym. Chem.* **1992**, *30*, 337.
(30) de Gennes, P. G. *Mol. Cryst. Liq. Cryst.* **1984**, *102*, 95.
(31) Abe, A. *Macromolecules* **1984**, *17*, 2280.
(32) Yoon, D. Y.; Bruckner, S. *Macromolecules* **1985**, *18*, 6651.
(33) Blumstein, R. B.; Blumstein, A. *Mol. Cryst. Liq. Cryst.* **1988**, *165*, 361.
(34) Lehmann, O. *Uber Physikalische Isomerie*; from Kelker, H., 1877. History of Liquid Crystals. *Mol. Cryst. Liq. Cryst.* **1973**, *21*, 1.
(35) Percec, V.; Keller, A. *Macromolecules* **1990**, *23*, 4347.
(36) Volander, D. *The investigation of Molecular shape with the aid of liquid crystals*; communication from the Institute of Chemistry of Halle ADS, 1923.
(37) Percec, V.; Tsuda, Y. *Macromolecules* **1990**, *23*, 3509.
(38) Percec, V.; Yourd, R. *Macromolecules* **1989**, *22*, 524; 3229.
(39) Ungar, G.; Feijoo, J. L.; Keller, A.; Yourd, R.; Percec, V. *Macromolecules* **1990**, *23*, 244.
(40) Ungar, G.; Percec, V.; Zuber, M. *Macromolecules* **1992**, *25*, 1193.
(41) Cheng, S. Z. D.; Yandrasits, M. A.; Percec, V. *Polymer* **1991**, *32*, 1284.
(42) Yandrasits, M. A.; Cheng, S. Z. D.; Zhang, A.; Cheng, J.; Wunderlich, B.; Percec, V. *Macromolecules* **1992**, *25*, 2112.
(43) Cheng, J.; Jing, Y.; Wunderlich, B.; Cheng, S. Z. D.; Yandrasits, M. A.; Zhang, A.; Percec, V. *Macromolecules*, in press.
(44) Adduci, J.; Lenz, R. W. Manuscript in preparation.
(45) Avrami, M. *J. Chem. Phys.* **1939**, *7*, 1109; **1940**, *8*, 212; **1941**, *9*, 117.
(46) Chandrasekher, S. *Liquid Crystals*; Cambridge University Press: London, 1977.
(47) Pershan, P. S. *Structure of Liquid Crystal Phase*; World Scientific: Singapore, 1988.
(48) Pardey, R. Ph.D. Dissertation, Department of Polymer Science, The University of Akron, Akron, OH 1993.
(49) Keller, A. In *Polymers, Liquid Crystals and Low-Dimensional Solids*; March, N., Tosi, M., Eds.; Plenum: New York and London, 1984.
(50) Wunderlich, B.; Grebowicz, J. *Adv. Polym. Sci.* **1984**, *60/61*, 1.